Supplemental Data

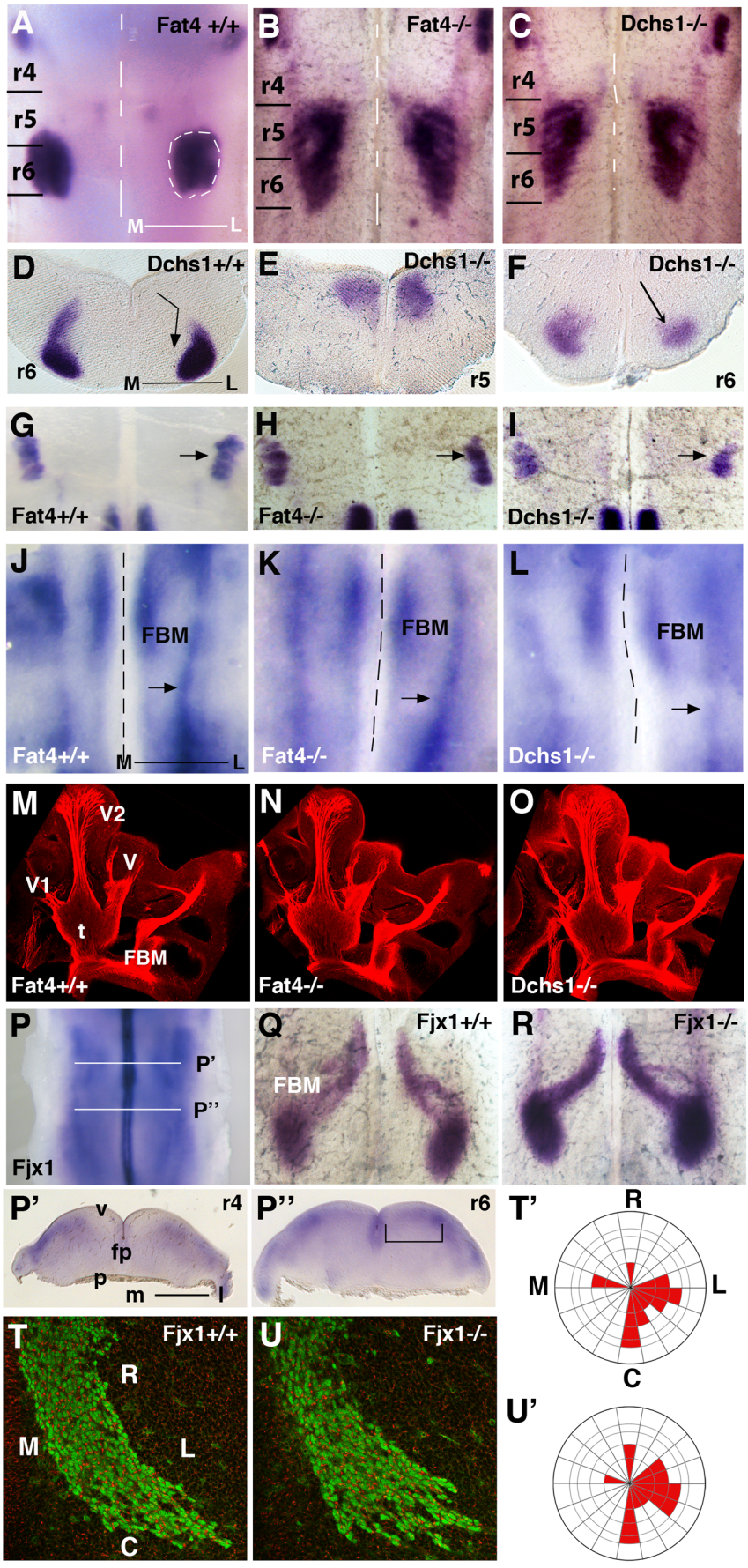
A
Fat4 +/+
r4
r5
r6
M
L
B
Fat4-/-
r4
r5
r6
C
Dchs1-/-
r4
r5
r6
D
Dchs1+/+
r6
M
L
E
Dchs1-/-
r5
F
Dchs1-/-
r6
G
Fat4+/+
H
Fat4-/-
I
Dchs1-/-
J
FBM
Fat4+/+
M
L
K
FBM
Fat4-/-
L
FBM
Dchs1-/-
M
V2
V
V1
t
FBM
Fat4+/+
N
Fat4-/-
O
Dchs1-/-
P
P'
P''
Fjx1
Q
Fjx1+/+
FBM
R
Fjx1-/-
P'
v
r4
fp
p
m
l
P''
r6
T'
R
M
L
C
T
Fjx1+/+
R
M
L
C
U
Fjx1-/-
U'

Figure S1 The migratory defect is specific to the facial branchiomotor neurons, related to Figure 1

Flat-mounts (A-C, G-L) and sections (D-F) through wildtype (A,D,G,J), *Fat4*$^{-/-}$ (B, H, K), *Dchs1*$^{-/-}$ (C, F, I, L) hindbrains whole-mounted for Islet1 (A-I), and semaphorin 3A (J-L) at stage E11.5 (G-L), E13.5 (D-F) and E14.5 (A-C). In *Fat4*$^{-/-}$ and *Dchs1*$^{-/-}$ hindbrains the FBM neurons fail to undertake the lateral tangential migration below the ventricular surface (E) and finally take an abnormal radial trajectory towards the pial surface to form a nucleus closer to the midline (F compare with D, also compare A with B,C). The trigeminal and glossopharyngeal neurons are indicated by black arrows in (G-I) and (J-L) respectively and migrate normally. The midline is shown by a dashed line in (A-C, J-L). (M-O) Immunolabelling of the cranial axons in wildtype (M), *Fat4*$^{-/-}$ (N) and *Dchs1*$^{-/-}$ (O) E11.5 embryos also indicates that rhombomere and neuronal identity are unaffected in *Fat4*$^{-/-}$ and *Dchs1*$^{-/-}$ mutants. (P) shows *in situ* hybridisation of *Fjx1* expression within an E12.5 hindbrain; P is a flatmount view; P' and P'' are sections through r4 and r6 respectively. The area above the bracket in P'' shows the region of FBM medio-lateral migration. (Q-U) show an *in situ* hybridization (Q,R) and Islet1(green)/Golgi(red) immunostaining (T,U) of the FBM neurons at E12.5 in *Fjx1*$^{+/+}$ (T) and *Fjx1*$^{-/-}$ (U) E12.5 embryos. (T',U') show the corresponding Rose plots of Golgi polarity within the FBM neurons. fp, floor plate; FBM, facial branchiomotor neuron; m-l, medial-lateral; p, pial layer of hindbrain; r, rhombomere: V, V1,V2 subdivisions of the trigeminal nerve (t); v, ventricular layer of hindbrain.

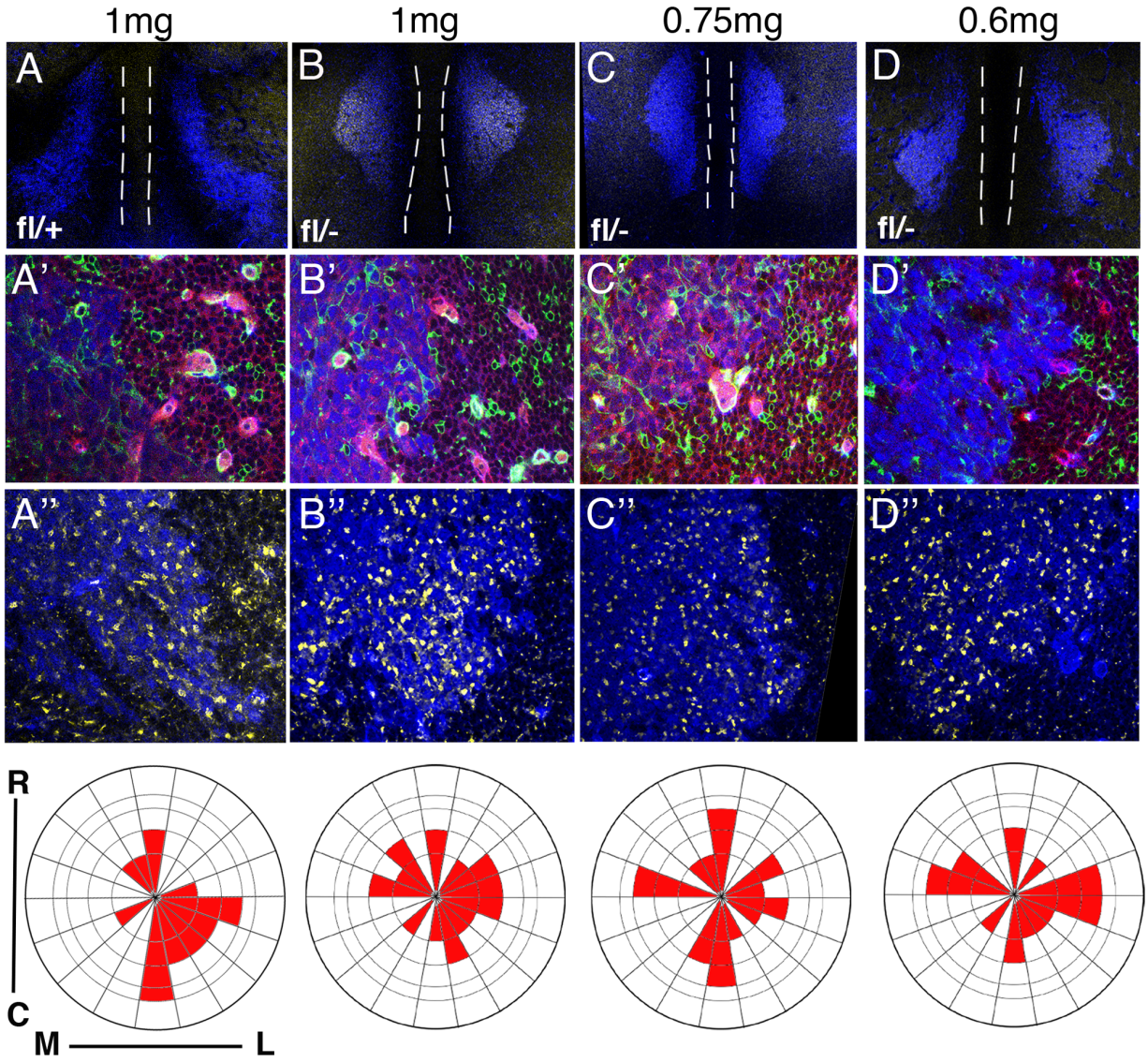
1mg
1mg
0.75mg
0.6mg
A
B
C
D
fl/+
fl/-
fl/-
fl/-
A'
B'
C'
D'
A''
B''
C''
D''
R
C
M
L

Figure S2. Mosaic disruption of Dchs1 function indicates that Dchs1 controls FBM neuronal migration via PCP, related to Figure 3

(A-D) show the effect of different tamoxifen doses i.e. mosaicism on FBM (blue, Islet1 immunostaining) neuronal migration in a *Dchs1*$^{f/+}$ (A) or *Dchs1*$^{f/-}$ background (B-D). (A'-D' and A''-D'') show higher power views also revealing Cre mosaicism (green) in a tomato background (red) and Golgi (yellow) immunostaining respectively. Golgi polarity is quantified in the Rose plots below. The dashed lines in (A-D) indicate the midline of the hindbrain to show the extent of lateral migration.

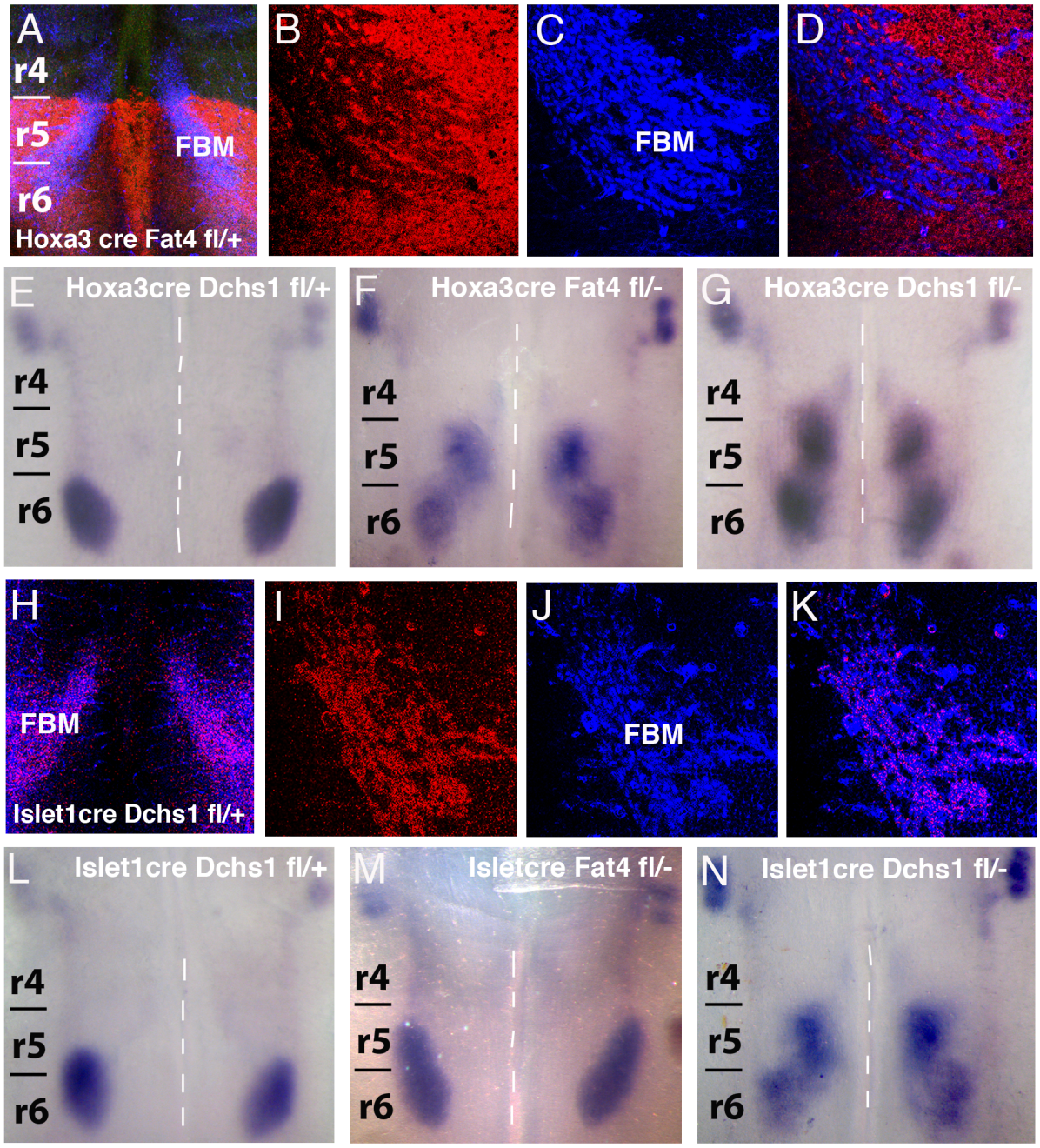
A
r4
r5
r6
FBM
Hoxa3 cre Fat4 fl/+
B
C
FBM
D
E
Hoxa3cre Dchs1 fl/+
r4
r5
r6
F
Hoxa3cre Fat4 fl/-
r4
r5
r6
G
Hoxa3cre Dchs1 fl/-
r4
r5
r6
H
FBM
Islet1cre Dchs1 fl/+
I
J
FBM
K
L
Islet1cre Dchs1 fl/+
r4
r5
r6
M
Isletcre Fat4 fl/-
r4
r5
r6
N
Islet1cre Dchs1 fl/-
r4
r5
r6

Figure S3. Fat4 and Dchs1 regulate PCP by both cell autonomous and non-cell autonomous mechanisms, related to Figure 2

(A-G) Hoxa3^{Cre} inactivation of Fat4 and Dchs1 expression within r5 and r6 in the neuroepithelium. (H-N) Islet1^{Cre} inactivation of Fat4 and Dchs1 expression within the FBM neurons. (A-D and H-K) show Cre-inactivation: Cre activity and FBM neurons are indicated by immunolabelling for β-galactosidase (Red, A,B,H,I) and Islet1 (Blue, A,C,H,J) antibody staining respectively. (A, H) are low power views, (D, K), merged pictures of (B,C) and (I, J) respectively. (E-G) and (L-N) *in situ* hybridisation of *Islet1* expression revealing impaired FBM neuronal migration at E13.5 following Cre inactivation of Fat4 (F, M) or Dchs1 (G,N) within the neuroepithelium (F,G) or FBM neurons (M,N). The midline is indicated by dashed lines. r4-r6, rhombomeres 4-6

Supplemental Experimental Procedures

Mice

All mouse procedures were approved by University of Medicine and Dentistry, New Jersey, USA, Institutional Animal Care and Use Committee or King's College London, UK in accordance with established guidelines for animal care. The day of the mouse plug was assigned E0.5. The following mouse lines were used: Fat4 [S1], Dchs1 [S2], *Vangl2^{Lp}* [S3], Hoxa3$^{tm1(cre)Moon}$ [S4], Islet1$^{tm1(cre)Sev}$ [S5], Gt(ROSA)26Sor^{tm1Sor} [S6], Gt(ROSA)26Sor$^{tm4(ACTB-tdTomato-EGFP)Luo}$ (mT/mG) [S7], Gt(ROSA)26Sor$^{tm1(cre/ERT2)Tyj}$/J [S8]. The Dchs1$^{f/f}$ allele and Fat4$^{f/f}$ allele were made in the laboratories of Ken Irvine and Helen McNeill respectively. Dchs1 conditional embryos and Fat4 conditional embryos were generated by mating Dchs1$^{f/f}$R26R$^{LacZ/LacZ}$ or Fat4$^{f/f}$R26R$^{LacZ/LacZ}$ females with Islet1$^{cre-Sev}$ Dchs1 (or Fat4)$^{+/-}$ and

Hoxa3$^{cre\text{-}Moon}$ Dchs1(or Fat4)$^{+/-}$ males. Tamoxifen inducible mosaic embryos in heterozygous background were generated by mating Dchs1$^{f/f}$ R26$^{mT/mG}$ line with Cre-ER^{TM}Dchs1$^{+/-}$ line. For mosaic embryos in the wildtype background Dchs1$^{f/f}$ R26$^{mT/mG}$ animals were mated to Cre-ER^{TM}Dchs1$^{f/f}$ mice. All tamoxifen (Sigma-Aldrich T5648) injections were performed at E10.5.

PCR genotyping

DNA was isolated using Direct PCR-Ear Lysis reagent (PeqLab) and genotyping was performed by PCR using allele-specific primers. Genotyping of Fat4 and Dchs1 mice was performed as previously described [S2]. Genotyping of *Vangl2*^{Lp} mice was performed according to [S9]. The following primers were used for genotyping the other lines: Fat4$^{f/f}$ (Fwd: 5' GAGTGCAACAAGATATGGTGGC3', Rev: 5'TACAGGGAACAAAGGTGCTGAG3') generating 2 products of 0.3kb for wt allele and 0.45kb for the flox allele; Dchs1$^{f/f}$ (Fwd: 5' CCCCCAGACATTCTCAGCCCTTCTTCTA3', Rev 5' CACAGGGCCAGCAGCTCATCCATTT 3') giving a product of 0.67kb for Wt allele and 0.77kb for flox allele; R26R^{WT} allele (Fwd, 5'AAGTCGCTCTGAGTTGTTAT3', Rev, 5'GGAGCGGGAGAAATGGATATG3') generating product of 0.6kb; R26R^{LacZ} allele (Fwd: 5' AAGTCGCTCTGAGTTGTTAT3', Rev: 5' GCGAAGAGTTTGTCCTCAACC3') giving product of 0.3kb; mT/mG allele was detected using primers (Fwd: 5' CTCTGCTGCCTCCTGGCTTCT3', Rev: 5'TCA ATG GGCGGGGGTCGTT3') which generated product of 0.25kb for mT/mG allele and (Fwd, 5' CTCTGCTGCCTCCTGGCTTCT3', Rev: 5' CGAGGCGGATCACAAGCAATA3') to detect a product of 0.33kb for Wt allele. All the Cre lines were genotyped using primers (Fwd: 5' CCTGGAAAATGCTTCTGTCCG3', Rev: 5' CAGGGTGTTATAAGCAATCCC3') giving a product of 0.39kb. For each gene, amplification was performed for 35 cycles, annealing

temperatures were 57°C for *Fat4* and 59°C for the remaining genes. The PCR products were visualized on an 1.5% agarose gel.

Statistical and Image analysis

The significance of the Golgi apparatus polarisation within the FBM neurons was determined by the Rayleigh test [S10]. A value of $p<0.05$ indicates a significant polarisation. To determine if the distribution of the Golgi polarisation was significantly different between control and mutant FBM neurons, the Mardia-Watson-Wheeler test [S10] was performed. A value of $p <0.05$ indicates a significant difference. To quantify levels of expression following immunolocalisation of Fat4 and Dchs1, an ImageJ line plot tool was used to measure pixel intensity.

Immunofluorescent staining and imaging

Hindbrains were fixed in 4% paraformaldehyde overnight and then washed five times with PBST (PBS, 0.2%TritonX-100, 1%BSA) for 1 hour at room temperature. The hindbrains were blocked with 5% donkey serum in PBST (PBST-serum) for 5 hours at room temperature, and then incubated with primary antibodies in PBST-serum for two to three days at 4ºC before washing with PBST for 1 hour at room temperature, five times. Hindbrains were then incubated with secondary antibodies in PBST-serum for two to three days at 4ºC, and washed as for primary antibodies, plus an additional 12 to 36-hour wash. Nuclei were counter-stained with Hoechst. For Phalloidin staining, hindbrains were incubated in Alexa Fluor 647-Phalloidin (1 in 100 dilution, Invitrogen) in PSBT-serum for three days at 4ºC. Stained hindbrains were mounted in Vectashield mounting medium (Vector Labs) and imaged using a Leica SP5 confocal microscope. Primary antibodies used were rabbit anti-Dchs1 (1:200) and anti-Fat4 (1:200) [S11], mouse anti-Islet1(DSHB, 1:400), rabbit anti-Giantin (Abcam, ab24568, 1:1000), and chick anti-beta-galactosidase (Abcam, ab9361, 1:400). Axon Neurofilament staining was carried out to

whole embryos as described by [S12] using antibody against neurofilament protein (gift from Dr. Ivo Liebram, King's College London). Golgi polarity was determined by analyzing the 3D confocal stacks of the Islet1/Golgi immunostained FBM neurons so that for each cell the Golgi and the corresponding nucleus could be identified. A line was drawn through the Golgi apparatus to the base of the nucleus and the angle of this line relative to the midline of the hindbrain was plotted in Rose plots.

The numbers of mutant embryos together with the corresponding controls, analysed for each stage and study are as follows; Islet1 expression and Golgi immunolocalisation: E12.5: Fat4, n=3, Dchs1, n=3, $Hox3^{cre}Fat4^{f/f}$, n=3, $Islet1^{cre}Fat4^{f/f}$, n=4, $Hoxa3^{cre}Dchs1^{f/f}$, n=3, $Islet1^{cre}Dchs1^{f/f}$, n=3, mT/mG$Dchs1^{f/+}$, n=3 at each dose; mT/mG$Dchs1^{f/f}$, n=3. Islet immunolocalisation alone: $Fat4^{-/-}$/$Vangl2^{Lp/Lp}$, E12.5, n=2, E13.5, n=3; Fat4, E11.5, n=3; Dchs1, E11.5, n=4; Phalloidin, staining E12.5, Dchs1, n=3.

In situ hybridisation

Heads from E10.5-E14.5 embryos were fixed in 4% paraformaldehyde at 4ºC overnight and then dehydrated into methanol and stored at -20C. *In situ* hybridization was carried out according to [S2] using the following probes: Rat Islet1**(**Addgene, 16238); Hoxb1 [S13]; Tbx20 [S14]; Cadh-8 [S15]; Sema3A [S16] ; EphA4 [S17]; Neogenin [S18]; Ret [S19] . The numbers of $Fat4^{-/-}$ and $Dchs1^{-/-}$ embryos, together with the corresponding $Fat4^{+/+}/Dchs1^{+/+}$ or $Fat4^{+/-}/Dchs1^{+/-}$embryos, analysed for each probe are as follows: Islet1 (Fat4: E11.5, n=3; E12.5, n=4; E13.5, n=3; E14.5, n=2; Dchs1: E11.5, n=3; E12.5, n=7; E13.5, n=5; E14.5, n=2; $Fat4^{-/-}$/$Dchs1^{-/-}$, E12.5, n=3; $Fat4^{-/-}$/$Vangl2^{Lp/Lp}$, E13.5, n=2). Hoxb1: E10.5, Fat4, n=2; Dchs1, n=2; EphA4: E10.5, Fat4, n=2; Dchs1, n=2; Tbx20 E12.5, Fat4, n=2; Dchs1, n=2; Cadh-8 E12.5, Fat4, n=2; Dchs1, n=2; Sema3A, E11.5: Fat4, n=2; Dchs1, n=2.

Quantitative PCR

RNA was isolated from E12.5 hindbrains using TRIzol Reagent (Invitrogen) according to manufacturer's instructions. cDNA was made from 200 ng total RNA as a template using Precision nanoScript Reverse Transcription Kit (Primer Design). QPCR for Dchs1 mRNA expression, and GAPDH as a control, was performed in triplicate using Precision real-time PCR MasterMix with SYBR green by Primer Design as per manufacturer's instructions using the following primers: Dchs1Fwd 5'GGCCTGCCTCCTTTAGTCTC3'; Dchs1Rev, 5'TGTCAGCATCTGTGGCTGTT3'; GAPDHFwd, 5' AGGTCGGTGTGAACGGATTTG3'; GAPDHRev, 5'TGTAGACCATGTAGTTGAGGTCA 3'. Quantitative PCR was performed and analysed using a Qiagen Rotor-Gene Q machine and software package. Data was quantified using the Delta-delta CT method.

Supplemental References

S1. Saburi, S., Hester, I., Fischer, E., Pontoglio, M., Eremina, V., Gessler, M., Quaggin, S.E., Harrison, R., Mount, R., and McNeill, H. (2008). Loss of Fat4 disrupts PCP signaling and oriented cell division and leads to cystic kidney disease. Nat Genet *40*, 1010-1015.

S2. Mao, Y., Mulvaney, J., Zakaria, S., Yu, T., Morgan, K.M., Allen, S., Basson, M.A., Francis-West, P., and Irvine, K.D. (2011). Characterization of a Dchs1 mutant mouse reveals requirements for Dchs1-Fat4 signaling during mammalian development. Development *138*, 947-957.

S3. Copp, A.J., Checiu, I., and Henson, J.N. (1994). Developmental basis of severe neural tube defects in the loop-tail (Lp) mutant mouse: use of microsatellite DNA markers to identify embryonic genotype. Dev Biol *165*, 20-29.

S4. Macatee, T.L., Hammond, B.P., Arenkiel, B.R., Francis, L., Frank, D.U., and Moon, A.M. (2003). Ablation of specific expression domains reveals discrete functions of ectoderm- and endoderm-derived FGF8 during cardiovascular and pharyngeal development. Development *130*, 6361-6374.

S5. Yang, L., Cai, C.L., Lin, L., Qyang, Y., Chung, C., Monteiro, R.M., Mummery, C.L., Fishman, G.I., Cogen, A., and Evans, S. (2006). Isl1Cre reveals a common Bmp pathway in heart and limb development. Development *133*, 1575-1585.

S6. Soriano, P. (1999). Generalized lacZ expression with the ROSA26 Cre reporter strain. Nat Genet *21*, 70-71.

S7. Muzumdar, M.D., Tasic, B., Miyamichi, K., Li, L., and Luo, L. (2007). A global double-fluorescent Cre reporter mouse. Genesis *45*, 593-605.

S8. Ventura, A., Kirsch, D.G., McLaughlin, M.E., Tuveson, D.A., Grimm, J., Lintault, L., Newman, J., Reczek, E.E., Weissleder, R., and Jacks, T. (2007). Restoration of p53 function leads to tumour regression in vivo. Nature *445*, 661-665.

S9. Vladar, E.K., Bayly, R.D., Sangoram, A.M., Scott, M.P., and Axelrod, J.D. (2012). Microtubules enable the planar cell polarity of airway cilia. Curr Biol *22*, 2203-2212.

S10. Mardia, K.V., Jupp, P.E., and Mardia, K.V.S.o.d.d. (2000). Directional statistics, [New ed.] Edition, (Chichester: Wiley).

S11. Ishiuchi, T., Misaki, K., Yonemura, S., Takeichi, M., and Tanoue, T. (2009). Mammalian Fat and Dachsous cadherins regulate apical membrane organization in the embryonic cerebral cortex. J Cell Biol *185*, 959-967.

S12. McNeill, E.M., Roos, K.P., Moechars, D., and Clagett-Dame, M. (2010). Nav2 is necessary for cranial nerve development and blood pressure regulation. Neural development *5*, 6.

S13. Wilkinson, D.G., Bhatt, S., Cook, M., Boncinelli, E., and Krumlauf, R. (1989). Segmental expression of Hox-2 homoeobox-containing genes in the developing mouse hindbrain. Nature *341*, 405-409.

S14. Kraus, F., Haenig, B., and Kispert, A. (2001). Cloning and expression analysis of the mouse T-box gene tbx20. Mech Dev *100*, 87-91.

S15. Korematsu, K., and Redies, C. (1997). Restricted expression of cadherin-8 in segmental and functional subdivisions of the embryonic mouse brain. Dev Dyn *208*, 178-189.

S16. Melendez-Herrera, E., Colin-Castelan, D., Varela-Echavarria, A., and Gutierrez-Ospina, G. (2008). Semaphorin-3A and its receptor neuropilin-1 are predominantly expressed in endothelial cells along the rostral migratory stream of young and adult mice. Cell Tissue Res *333*, 175-184.

S17. Gilardi-Hebenstreit, P., Nieto, M.A., Frain, M., Mattei, M.G., Chestier, A., Wilkinson, D.G., and Charnay, P. (1992). An Eph-related receptor protein tyrosine kinase gene segmentally expressed in the developing mouse hindbrain. Oncogene *7*, 2499-2506.

S18. Keeling, S.L., Gad, J.M., and Cooper, H.M. (1997). Mouse Neogenin, a DCC-like molecule, has four splice variants and is expressed widely in the adult mouse and during embryogenesis. Oncogene *15*, 691-700.

S19. Pachnis, V., Mankoo, B., and Costantini, F. (1993). Expression of the c-ret proto-oncogene during mouse embryogenesis. Development *119*, 1005-1017.